Color Micropatterning with Reconfigurable Stamps

A. Bitner, M. Fiałkowski, and B. A. Grzybowski*

Department of Chemical and Biological Engineering, Northwestern University, 2145 Sheridan Rd., Illinois 60208

Received: September 30, 2004; In Final Form: November 9, 2004

A two-phase, reaction−diffusion (RD) system is described in which printing stamps of the same geometries produce different micropatterns when applied to different surfaces. Initial outflow of water from an agarose stamp into a dry gelatin "paper" causes redistribution of a chemical "ink" contained in the stamp. Depending on the gelatin's water absorptivity, the ink is printed at different locations and develops into different types of color patterns. The mechanism of formation of these patterns is studied using stamps with polygonal tiling surface reliefs. Scaling arguments are derived that explain formation of different pattern types for different geometrical parameters of the system.

Adaptive systems,[1,2] that is systems whose structure and function change autonomously in response to the changes in the environment, are not only of fundamental interest for their relevance to life but are also promising candidates for "intelligent" materials,[3] devices[4] and technological processes.[5] While nature uses adaptability routinely,[6−8] there are only a handful of examples of artificial physicochemical ensembles that would be able to "reconfigure" themselves and perform different useful operations upon receiving different external stimuli.[9−11] Here, we describe a two-phase reaction−diffusion (RD)[12−14] system for color micropatterning of surfaces, in which a printing stamp reconfigures itself in response to the properties of the surface onto which it is applied. In this system, an agarose stamp having a network of connected, microscopic features in bas relief and uniformly soaked in a solution of iron(III) chloride (an "ink") is placed onto a thin layer of dry gelatin uniformly doped with potassium hexacyanoferrate, $K_4[Fe(CN)_6]$. Depending on the dimensions of the system, the gelatin "paper" drains different amounts of water from different parts of the network, thus establishing concentration gradients of the Fe^{3+} cations left therein. In response to these gradients, the cations redistribute within the network and enter the gelatin either from the network's edges or from its nodes to produce different color patterns upon reaction with $[Fe(CN)_6]^{4-}$ anions; stamps of the same geometries print different patterns depending on the absorptivity of the "paper" onto which they are printed (Figure 1). In regular, polygonal networks, the color patterns that emerge are either the tile-centering (TC) or dual lattice (DL) transformations[15] of the stamped network, and the sharp transition between these two modes is governed by one dimensionless parameter.

Figure 1a outlines the experimental procedure described in detail elsewhere.[14,16] In short, an agarose stamp (8% w/w OmniPur Hi-Strength Agarose, Darmstadt, Germany) having a regular network of raised features ($h = 40$ μm; $d = 40$ to 150 μm; $L = 300$ to 1000 μm) embossed on its surface was uniformly soaked in a 10% w/w solution of ferric(III) chloride ($FeCl_3$) for 15 min. The stamp was then gently dried on a tissue paper for ∼30 s, and was brought into conformal contact with a thin ($H = 10$ to 40 μm) layer of the dry gelatin (Gelatin B, 225 bloom, Sigma-Aldrich) uniformly doped with film of 1% w/w of potassium hexacyanoferrate, $K_4[Fe(CN)_6]$.

Water from the stamp rapidly wetted the surface of the dry gelatin by capillarity (at a rate of several μm/s) and slowly diffused into its bulk ($D_w \sim 10^{-7}$ cm^2/s). The iron cations from the stamp were delivered diffusively into an already wetted, thin layer ($H_{eff} \sim 10$ μm)[14] of gelatin near the surface, where they reacted with hexacyanoferrate inions to give a deep-blue precipitate (Prussian Blue). As the cations diffused away from the features of the stamped network, they precipitated all $[Fe(CN)_6]^{4-}$ they encountered. The unconsumed hexacyanoferrate inions between the features experienced a sharp concentration gradient and diffused in directions opposite to the incoming reaction fronts (Figure 1a, bottom). Ultimately, when all hexacyanoferrate ions were consumed, propagation of the color fronts stopped to give thin, uncolored lines [14] delineating a new pattern in the gelatin film.

In this pattern, the uncolored lines could either bisect the angles between the crossing features of the stamped network or could run perpendicular to its edges (Figure 1c, 2). In particular, when the stamped network was a regular, polygonal tiling, the pattern emerging in the gelatin could be either its TC or DL transformation depending on the dimensions of the system (Figure 2). We observed that the same stamps gave TC tilings when printed onto thinner gels and DL tilings when printed onto thicker ones (Figure 2c−e). In addition, for a given value of H, TC patterns developed from networks with thinner and/or longer edges, and DL patterns developed from networks with thicker and/or shorter edges (Figure 2b).[17]

These trends held for different geometries of the stamped networks and can be explained by a two-stage mechanism in which the initial (i.e., in the first 1−2 min, when the surface is wetted by capillarity) outflow of water from the features of the stamped network establishes concentration gradients within the network and determines the type of the resultant color tiling in gelatin.

Specifically, three interrelated effects need to be considered. (i) Diffusional closure of the features. As water flows out from the features into gelatin, a gradient of water concentration, ρ, is established in the vertical, z, direction; there is less water near the gelatin surface ($z \approx 0$) than at the bases of the features

* Corresponding author. E-mail: grzybor@northwestern.edu.

10.1021/jp045539o CCC: $27.50
Published on Web 12/04/2004

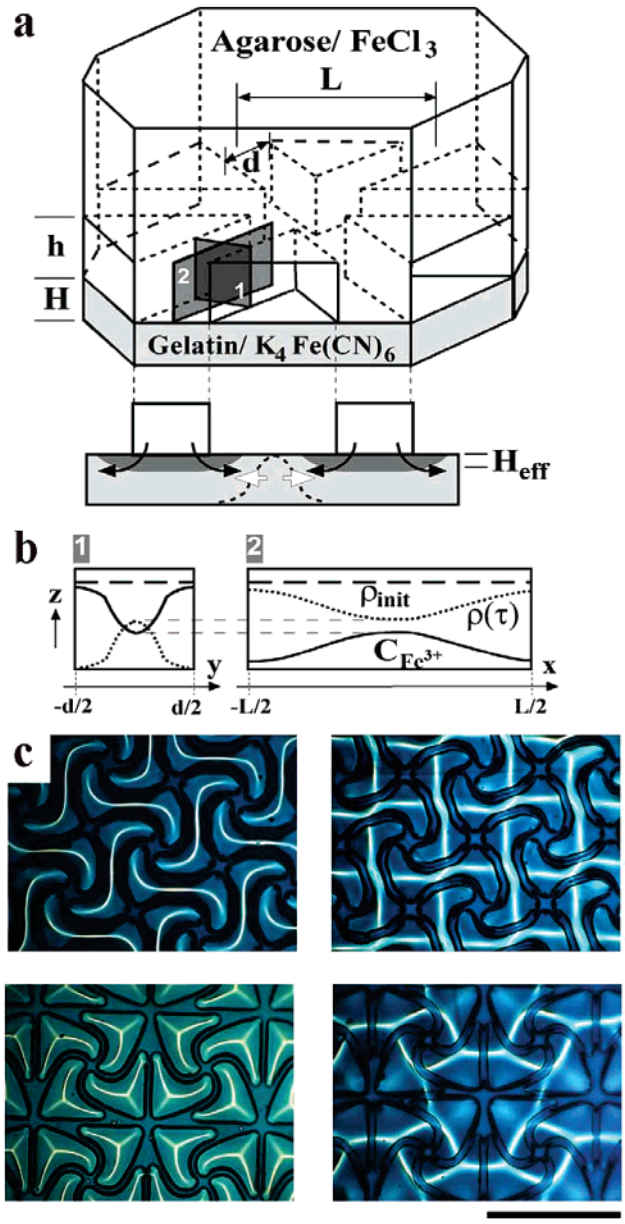

Figure 1. Adaptive printing. (a) (top) The scheme illustrates wet stamping of a network of connected features (here, triangular lattice) and defines pertinent dimensions. (bottom) Cross-sectional view of the edges of the stamped network. Solid arrows give approximate directions of diffusion of Fe^{3+} cations into gelatin and the white arrows give those of the hexacyanoferrate ions within gelatin. All ions migrate in a thin ($H_{eff} \approx 10\ \mu$m), wetted layer near the surface of gelatin. The dashed line illustrates the concentration gradient the $[Fe(CN)_6]^{4-}$ anions between the features experience, and along which they migrate. (b) Qualitative water-content and Fe^{3+}-concentration profiles across an edge (left), and along it (right). The numbers correspond to the shaded planes in (a). (c) Optical micrographs of different color patterns obtained from the same stamps on thin gels (left column, $H = 10\ \mu$m) and thick gels (right column, $H = 40\ \mu$m). The scale bar corresponds to 1 mm.

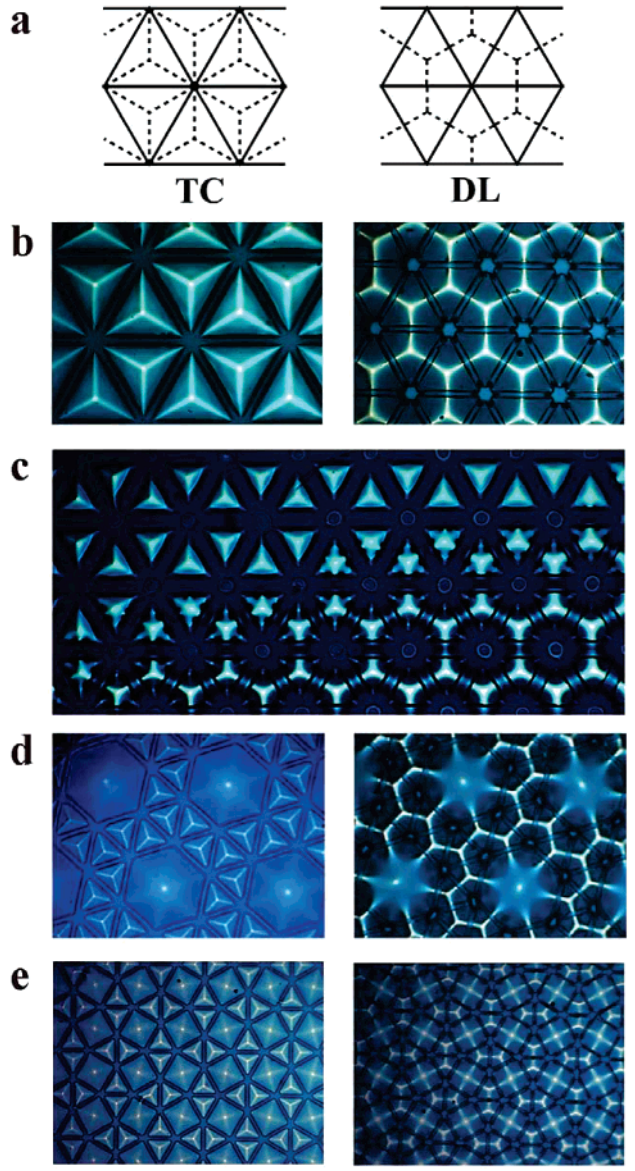

Figure 2. Color patterns developed from stamped polygonal lattices. (a) Definition of a tile-centered, TC, and a dual-lattice, DL, transformations (both dashed lines) of a stamped triangular network (solid lines). (b−e) TC and DL tiling transformations obtained from networks of different geometries and/or dimensions; all networks shown are examples of either Archimedean or Laves tilings; [15] all dimensions are in μm. (b) left: TC, equilateral triangles ($d = 50$, $L = 900$, $H = 40$); right: DL, equilateral triangles ($d = 50$, $L = 700$, $H = 40$). (c) Two solutions obtained from a network of equilateral triangles ($d = 50$, $L = 300$) on a gel of thickness continuously varying from $\sim$10 μm in the top-left corner (TC solution) to $\sim$35 μm in the bottom-right corner (DL solution). (d) and (e) Identical stamps give TC solutions when applied on thinner gels ($H = 10\ \mu$m; left column) and DL solutions on thicker gels ($H = 30\ \mu$m; right column). For both lattices $d = 40\ \mu$m and $L = 300\ \mu$m.

($z \approx h$). This gradient obstructs the passage of Fe_3^+ and, as we have shown previously,[18] only the cations originally contained in the features are ultimately transported into gelatin. (ii) Gradient of ρ along the cross-section of the edges. Because water flows out with different speeds from different parts of the stamped network, the gradient of water content is established within the network (i.e., in the horizontal direction). Along a cross-section of a feature (i.e., in the yz plane direction), the borderline region ($y \approx \pm d/2$) loses water more rapidly than the center of the edge (Figure 1c, left). To see this, consider a process of dehydration of a one-dimensional, permeable medium confined at the interval $-d/2 < y < d/2$. Assuming uniform initial concentration of water, ρ_{init}, along the y-direction and that the outflow occurs at a constant rate at the ends of the interval, the transfer of water through the medium can be described by the Darcy equation,[19] $\partial/\partial t\ \rho(y,t) = \partial/\partial y\ (K(y)\ \partial/\partial y\ p(y,t))$. By relating hydrostatic pressures $p(y,t)$ to water contents,[20] this equation can be simplified to $\partial/\partial t\ \rho(y,t) = \kappa\ \partial^2/\partial y^2\ \rho(y,t)$, where

κ is some constant, $\rho(y, t = 0) = \rho_{init}$ for $-d/2 < y < d/2$, and $\partial/\partial y\ \rho(y,t) =$ const for $y = \pm d/2$. This means that the process of dehydration is governed by the diffusion equation, whose solutions (for the particular initial/boundary conditions imposed)[21] are bell-shaped profiles of ρ symmetric around $y = 0$. (iii) Gradient of ρ along the edges. The closer an element of an edge is to a node, the less water it loses (Figure 1c, right). This follows from geometrical arguments. Namely, the direction of the flux, q, of water flowing out of the stamp is perpendicular to the borderline of the feature. Furthermore, because the underpressure exerted by the expanding front of water is everywhere the same, water flows out of the stamp at an approximately constant rate. Thus, the amount of water transferred from a given element of the feature is proportional to the density of the flux lines. Because this density is the lowest for the elements located at the nodes, the nodes lose less water than the centers of the edges.

Differences in the water content induce gradients of Fe^{3+} concentration within the network (i.e., drier regions correspond to higher local concentrations). The cations diffuse along these gradients, both toward the centers of the edges and along the edges, toward the nodes. At the same time, they diffuse into the bulk of the gel, but at the early stages of water outflow, the wetted (swollen) gelatin layer under the features is very thin and the diffusion into the bulk is small compared with the lateral migration of ions within the network.

If the water content in the middle of the edges does not drop significantly in the course of water outflow (surface wetting), almost all ferric ions manage to diffuse along lateral gradients from the edges to the nodes where they enter the gelatin layer, and from where they propagate to give a DL tiling. In contrast, if ρ drops to such an extent as to significantly lower the mobility of Fe^{3+} in the agarose matrix,[22,23] efficient lateral transport over large distances is not possible, and the cations remain in the edges of the network, from which they slowly diffuse into gelatin. After 2−3 min, the reaction/color fronts start propagating from the borders of the edges of a network to give a TC tiling. These effects are vividly illustrated by the experimental images in Figure 3 and were quantified based on a series of experiments in which we printed equilateral triangle tilings of different dimensions (with $d = 50-150\ \mu$m and $L = 300-1000\ \mu$m) onto gelatin layers of varying thicknesses ($H = 10-40\ \mu$m).

First, we define a critical concentration ρ^* at the center of an edge (i.e., along $y = 0$), such that if the water content ρ therein drops below ρ^*, the Fe^{3+} cations cannot escape from the edges to the nodes; in general, ρ^* is a function of H, d, and L. For given geometrical parameters of the stamp (i.e., d and L), the effect of H on the TC−DL transition can be explained by comparing the characteristic times of surface wetting and the characteristic times of cation migration in the network. We begin by noting that as water wets the gelatin's surface between the stamped features by capillarity, it also diffuses into the gelatin's bulk. Consequently, the wetting front drags behind itself a layer of water traveling under the surface. Because on thicker gels water penetrates deeper (cf. ref 16 for detailed discussion), we expect that the speed of the wetting front, v_{wet}, should decrease with H. This hypothesis was verified experimentally: using optical microscopy, we measured the speeds of the wetting fronts to be 2.3 μm/s for $H = 10\ \mu$m, 1.7 μm/s for $H = 20\ \mu$m, 1.1 μm/s for $H = 30\ \mu$m, and 0.9 μm/s for $H = 40\ \mu$m. During the wetting, $\rho(y = 0)$ decreases approximately linearly with time, and the amount of water lost by the features is proportional to the area of the wetted surface, $\rho_{init} - \rho(y = 0,\tau) \sim v_{wet}\ \tau$. Thus, the concentration of water at the center of an edge drops down to ρ^* after time $\tau_{closure}(H) \sim (\rho_{init} - \rho^*)/v_{wet}(H)$. The TC solution develops when iron cations are trapped in the edges, i.e., when $\tau_{esc} > \tau_{closure}$, where τ_{esc} is the characteristic time needed for iron cations to escape to the nodes; if $\tau_{esc} < \tau_{closure}$, DL pattern forms. Since τ_{esc} is independent of H, as it is roughly inversely proportional to the characteristic concentration gradient along the edge $\tau_{esc} \sim L/(\rho_{init} - \rho^*)$, the critical thickness, H^*, of the gel layer corresponding to the TC−DL transition is determined by $\tau_{closure}(H^*) = \tau_{esc}$. Thus, because

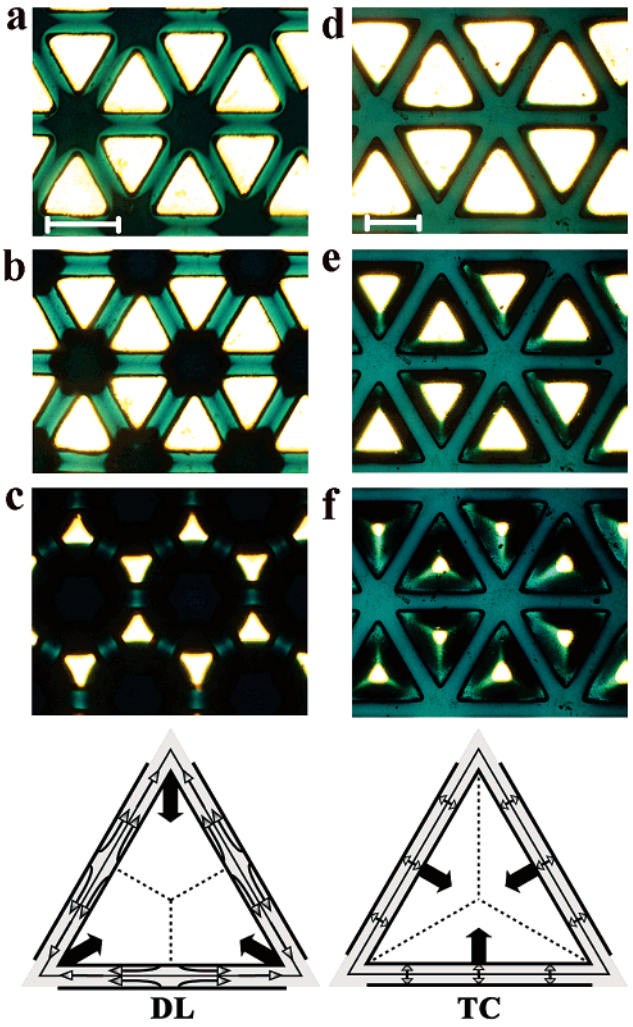

Figure 3. Snapshots of the stamp/gel interface developing into a DL tiling (left column, $d = 100\ \mu$m, $L = 400\ \mu$m, $H = 30\ \mu$m) and a TC tiling (right column, $d = 100\ \mu$m, $L = 700\ \mu$m, $H = 30\ \mu$m). The scale bar corresponds to 250 μm. The images are taken under intense illumination, which decomposes Prussian Blue to a greenish Berliner Yellow; this decomposition allows tracing the migration of Fe^{3+} ions. The initially dark-blue regions of the interface to which iron cations are not constantly being supplied fade; at the locations where the flux of Fe^{3+} persists, the interface remains deep blue. (a−c) In case of a DL solution, the ions leave the edges and travel along narrow "channels" toward the nodes, where 6-folded "stars" develop. These stars subsequently transform into regular hexagons and expand outward from the nodes. The interface under the edges does not regain the dark-blue color during the later stages of the process, indicating that the edges are completely depleted of Fe^{3+}. (d−f) In the case of a TC solution, the migration of ions along the edges is not observed. The interface below the edges remains uniformly colored during the initial surface wetting. Later, it becomes darker and the RD fronts start to propagate from the features' borderline. The diagrams at the bottom give the directions of flow of Fe^{3+} in agarose (thin arrows) and directions of the propagation of RD fronts in gelatin (thick arrows) for DL (left) and TC (right) solutions.

$v_{wet}(H)$ is a decreasing function of H, TC solutions develop on thinner gels (Figure 2d, e, left column), and DL solutions − on thicker ones (Figure 2d, e, right column). A striking manifestation of this effect is shown in Figure 2c in which the gel thickness increases continuously (∼10 μm/mm) from top-left to bottom-right, resulting in a crossover from TC to DL mode. Interestingly, the transition zone is fairly narrow (about 0.5 mm), which indicates that the system is very sensitive to the changes in H.

When the dimensions of the stamped array change and H are kept constant, the characteristic times $\tau_{closure}$ and τ_{esc} can be related to the geometrical parameters of the stamp. The closure time is estimated by equating the amount of water wetting the surface per unit time ($q \sim Lw_{eff}v_{wet}$, where w_{eff} is the thickness of the layer of water flooding the surface) to the amount of water released from the features per unit time. The latter quantity is found by approximating the cross-sectional water content of the features undergoing dehydration as a triangle (cf. Figure 1c, left), that is, $\rho \approx 0$ at $y = \pm d/2$, and $\rho = \rho(\tau)$ at $y = 0$, to obtain $q \sim -Ld\dot{\rho}$ ($y = 0,\tau$), where the dot stands for the time derivative. [24] Comparison of these two expressions yields $\rho_{init} - \rho(y = 0,\tau) \sim \tau w_{eff}v_{wet}/d$, and, consequently, $\tau_{closure} \sim d$. On the other hand, the escape time is proportional to the length of an edge, i.e., $\tau_{esc} \sim L$. This means that for a fixed thickness of the gel layer, the TC-DL transition is controlled by a dimensionless parameter $\eta = d/L$. The final pattern represents the TC transformation of the stamped network for $\eta < \eta^*$, and the DL transformation for $\eta > \eta^*$, where η^* is the critical value of η estimated as $\eta^* \sim \tau_{closure}/\tau_{esc} = 1$. This result agrees with experimental observations. We found that for $H = 30$ μm, the crossover between the TC and DL solutions was sharp and occurred at $\eta^* = 0.15 \pm 0.02$. When the gel thicknesses was varied, η^* decreased with increasing H (from 0.29 for H =10 μm to 0.06 at $H = 40$ μm).

In summary, we described a two-phase reaction−diffusion system in which the RD phenomena in one of the phases are coupled to and depend on the transfer of matter (here, water) between the phases. As a result of this coupling, the system shows bimodal behavior, which can be controlled precisely by the dimensions of the system. Since the stamps "feel" the properties of the support (e.g., absorptivity, thickness), they can potentially be used in sensory and analytical applications with easy geometrical readout.

Acknowledgment. B.G. gratefully acknowledges financial support from Northwestern University start-up funds and from the Camille and Henry Dreyfus New Faculty Awards Program. M.F. was supported by the NATO Scientific Fellowship.

References and Notes

(1) Adami, C. *Introduction to Artificial Life*; Springer-Verlag: New York, 1998.

(2) Chowhury, D.; Nishinari, K.; Schadschneider, A. *Phase Trans.* **2004**, *77*, 601.

(3) Hanselka, H. *Adv. Eng. Mater*. **2001**, *3*, 205.

(4) Kudryashov, A. V.; Seliverstov, A. V. *Optics Comm*. **1995**, *120*, 239.

(5) Boskovic, J. D. *AIChE J*. **1996**, *42*, 176.

(6) Bonabeau, E. *Ecosystems* **1998**, *1*, 437.

(7) Lippert, K.; Behn, U. *Annu. Rev. Comput. Phys*. **1997**, *5*, 287.

(8) Mangel, M. *J. Theor. Biol*. **2001**, *213*, 559.

(9) White, S. R.; Sottos, N. R.; Geubelle, P. H.; Moore, J. S.; Kessler, M. R.; Sriram, S. R.; Brown, E. N.; Viswanathan, S. *Nature* **2001**, *409*, 794.

(10) Runyon, M. K.; Johnson-Kerner, B. L.; Ismagilov, F. R. *Angew. Chem., Int. Ed.* **2004**, *43*, 1531.

(11) Julthongpiput, D.; Lin, Y. H.; Teng, J.; Zubarev, E. R.; Tsukruk, V. V. *J. Am. Chem. Soc.* **2003**, *125*, 15912.

(12) Zhabotinsky, A. M.; Zaikin, A. N. *Nature* **1970**, *225*, 535.

(13) Lengyel, I.; Epstein, I. R. *Science* **1991,** *251*, 650.

(14) Campbell, C. J.; Fialkowski, M.; Klajn, R.; Bensemann, I. T.; Grzybowski, B. A. *Adv. Mater*., **2004**, *16*, 1912.

(15) Grünbaum, B.; Shephard, G. C. *Tilings and Patterns*; Freeman: New York, 1986.

(16) Fialkowski, M.; Campbell, C. J.; Benseman, I. T.; Grzybowski, B. A. *Langmuir* **2004**, *20*, 3513.

(17) We note that when the stamps were sequentially applied onto different surfaces, they printed the patterns expected for a given surface provided that the time between consecutive stampings was longer than ∼1 min. In other words, after each printing, the stamps reconfigured back to the original, uniform distribution of water and reagents.

(18) Klajn, R.; Fialkowski, M.; Bensemann, I. T.; Bitner, A.; Campbell, C. J.; Bishop, K.; Smoukov, S.; Grzybowski, B. A. *Nature Mater.* **2004**, *3*, 729.

(19) Bird, R. B.; Steward, W. E.; Lightfoot, E. N. *Transport Phenomena*, 2nd ed.; Wiley: New York, 2001.

(20) Because the medium does not change its volume during the process, the changes in the hydrostatic pressure are due to the differences in local water concentration along the y direction, $p(y)$ is, approximately, a linear function of the deviation of $\rho(y)$ from its initial/equilibrium value, ρ_{init}, i.e., $p(y) \sim \rho_{init} - \rho(y)$; see, e.g., Flory, P. J. *Principles of Polymer Chemistry*; Cornell University: Ithaca, NY, 1953. We also assume that the changes of the permeability caused by the differences in the water content can be neglected.

(21) Crank, J. *The Mathematics of Diffusion*; Oxford University Press: Oxford, 2002.

(22) Valente, A. J. M.; Polishchuk, A. Y.; Lobo, V. M. M.; Geuskens, G. *Eur. Polym. J.* **2002**, *38*, 13.

(23) Krajewska, B. *React. Funct. Polym*. **2001**, *47*, 37.

(24) We note that the water content in the middle of an edge changes along the edge and is highest at the nodes and lowest in the middle.